

# A Sequential Quadratic Programming Approach to Combined Energy and Emission Management of a Heavy-Duty Parallel-Hybrid Vehicle<sup>★</sup>

S.C.M. Mennen, F.P.T. Willems, M.C.F. Donkers

*Eindhoven University of Technology, Netherlands*  
(e-mail: [sjoerd.mennen@gmail.com](mailto:sjoerd.mennen@gmail.com), [f.p.t.willems,m.c.f.donkers}@tue.nl](mailto:{f.p.t.willems,m.c.f.donkers}@tue.nl))

---

**Abstract:** Combined Energy and Emission Management (CEEM) problems are a class of optimal control problems that aim to minimize operational costs of (hybrid electric) powertrains with after-treatment system subject to constraints on emissions imposed by legislation. In this paper, a parallel-hybrid heavy-duty vehicle with a Variable Turbine Geometry (VTG) and an Exhaust-Gas Recirculation (EGR) system is considered. The CEEM problem is solved using Sequential Quadratic Programming (SQP) for which the powertrain and after-treatment models are approximated as smooth functions. It will be shown that solving the CEEM problem using SQP is computationally much more efficient when compared to other techniques like dynamic programming. It will also be shown that most of the benefits from CEEM come from the hybrid powertrain and not from regulating the VTG and ERG mass flows. Furthermore, zero emission zones and local emission constraints can also be included without too much effort.

*Keywords:* Nonlinear and Optimal Automotive Control, Engine Modelling and Control

---

## 1. INTRODUCTION

Hybrid vehicles are often associated with a positive impact on the environment due to the reduction of carbon emissions that they can achieve. At the same time, it is also possible to reduce the operating cost by driving (partially) electric. This optimal control of the power split between the fuel energy and the battery energy is known as energy management, see, e.g., (Khalik et al., 2018; Pérez et al., 2006; Onori and Serrao, 2011; Pisu and Rizzoni, 2007). Even though these energy management strategies achieve a reduction in carbon emissions, other harmful emissions such as nitrogen oxides (NO<sub>x</sub>) and particulate matter (PM) are ignored in (Khalik et al., 2018; Pérez et al., 2006; Onori and Serrao, 2011) or dealt with using constant weighting factors ignoring the dynamic behaviour of after-treatment systems (Pisu and Rizzoni, 2007). Still, modern emission legislation forces tailpipe emissions towards near-zero impact levels. A big problem within these energy management strategies is that there is an assumption that after-treatment systems operate under ideal circumstances, e.g., a warm start, whereas in the ‘real’ world these engines operate under cold-start conditions reducing the efficiency of the after-treatment system, which results in higher emission levels than expected (Muncrief, 2015). At the same time, the introduction of Zero-Emission Zones (ZEZs) will lead to driving electric for extended periods of time (Holmer et al., 2020; Demirgok et al., 2021), which results in cooling of the after-treatment system, thereby increasing emissions locally.

In order to deal with these effects, an optimal control problem can be formulated that aims at minimizing the operating cost subject to constraints on NO<sub>x</sub> emissions. This problem is known as Integrated Emission Management (IEM) or Combined Energy and Emission Management (CEEM), see (Donkers et al., 2017; Ao et al., 2008; Willems et al., 2011; Kessels et al., 2010). This CEEM problem has been solved using Dynamic Programming (DP) in (Donkers et al., 2017; Ao et al., 2008), Pontryagin’s Maximum Principle (PMP) and Equivalent Consumption Minimization Strategies (ECMS) in (Willems et al., 2011; Kessels et al., 2010). Although all methods yield a solution to the problem, there are some disadvantages. For example, the final solution presented in (Donkers et al., 2017) took 19 hours to compute for a drive cycle of 30 minutes. Even though computation time is not crucial when used for offline optimization, it shows that DP approaches do not scale well with horizon length and number of states/decision variables and cannot be applied to more complex problems. PMP or ECMS can, in principle, handle the required computational complexity. The problem with PMP for the CEEM problem is that a Two-Point Boundary Value Problem has to be solved while the differential equation involved for the controller states is typically unstable. To deal with this instability a pragmatic approach using heuristic rules is usually taken, resulting in techniques similar to ECMS, which then results in a sub-optimal solution.

This paper proposes to solve the CEEM problem using a static optimization approach. This is done using Sequential Quadratic Programming (SQP) (Nocedal and Wright, 2006). SQP aims to solve the non-linear CEEM problem by recursively solving linear constrained quadratic programs. SQP has already been proven suitable for energy man-

---

<sup>★</sup> This work has received financial support from the Horizon 2020 programme of the European Union under the grants ‘Efficient and environmental friendly LONG distance powertrain for heavy duty trucks and coaches’ (LONGRUN-874972).

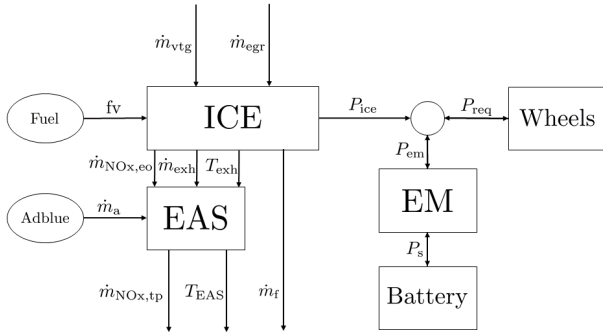


Fig. 1. Schematic of the considered system architecture.

agement strategies (Khalik et al., 2018) where optimality was obtained without significant computational effort. In this paper, we consider a case study of a parallel-hybrid heavy-duty vehicle with a variable turbine geometry and an exhaust-gas recirculation system, where the powertrain and aftertreatment models (which are typically expressed in lookup tables obtained from measurement data) are approximated as smooth functions. Simulation results show that the static optimization approach leads to favorable computation performance, and can handle ZEZs and local emission limits without much additional effort.

## 2. PROBLEM FORMULATION

The goal of this paper is to show that Sequential Quadratic Programming (SQP) can be used to solve the Combined Energy and Emission Management (CEEM) problem within a reasonable amount of time. To do so, a case study of a heavy-duty parallel-hybrid vehicle is considered. We first discuss the system architecture, powertrain and aftertreatment models under consideration and, subsequently, formulate the CEEM problem as an optimal control problem.

### 2.1 System Architecture

Fig. 1 shows a schematic representation of the considered architecture. As can be seen from this figure, a heavy-duty Internal Combustion Engine (ICE) is considered that works in parallel with an Electric Motor (EM) to provide the required torque and speed to the wheels. In the system, an Engine Aftertreatment System (EAS) is also present, which converts a mixture of the NOx and added Adblue to nitrogen and water vapour, thereby reducing the NOx tailpipe emissions.

Both the ICE and EM are seen as quasistatic models with a direct mapping from inputs to outputs. The model of the ICE then gives a mapping from the fuel value (fv) which gives the amount of fuel injected per cylinder per stroke cycle, and the mass flows  $\dot{m}_{vtg}$  and  $\dot{m}_{egr}$ , resulting from the Variable Turbo Geometry (VTG) and Exhaust-Gas Recirculation (EGR), respectively, to the output power  $P_{ice}$ , the engine-out NOx flow  $\dot{m}_{NOx,eo}$ , the exhaust mass flow  $\dot{m}_{exh}$ , the exhaust gas temperature  $T_{exh}$ , and the fuel consumption  $\dot{m}_f$ . The EM describes the quasistatic mapping from the power supplied from the battery  $P_s$ , to the resulting power from the EM  $P_{em}$ .

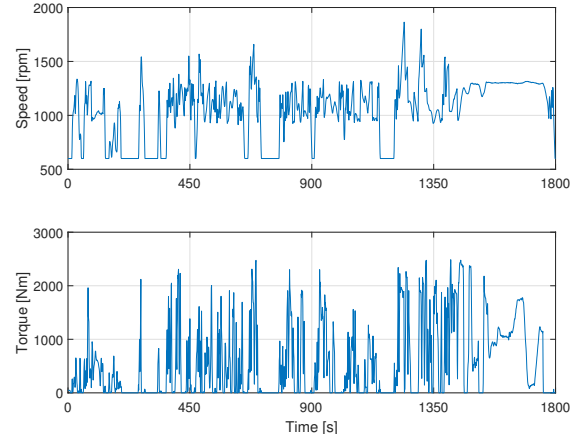


Fig. 2. World Harmonized Transient Cycle.

The EAS is modelled as a dynamic system, which will be discussed below. The inputs to this model are the engine-out NOx flow  $\dot{m}_{NOx,eo}$ , exhaust mass flow  $\dot{m}_{exh}$  and exhaust gas temperature  $T_{exh}$ , and the outputs are the tailpipe emissions  $\dot{m}_{NOx,tp}$ , and EAS temperature  $T_{EAS}$ . Note that, even though the Adblue consumption  $\dot{m}_a$ , is sketched as an input in Fig. 1, it is only considered to be a cost as Adblue consumption is assumed to be controlled as a function of engine-out NOx under the assumption that there is no ammonia storage in the selective catalytic reduction system of the EAS and the conversion is stoichiometric.

In this paper, we consider the World Harmonized Transient Cycle (WHTC) as an engine cycle, which is given in Fig. 2. When evaluating the NOx emissions on an engine test setup, usually two cycles are run: one with a cold start and one with a warm start. Since the cold start is the more challenging case, we focus on this case in this paper. Note that the required torque from the WHTC is always positive and, hence, this paper does not factor in any possibilities for regenerative braking using the EM. This means that any achievement in cost reduction is a result of better thermal management and not of regenerative braking.

### 2.2 Powertrain Modelling

The required driving power is determined by the WHTC and is given by

$$P_{req} = \frac{2\pi}{60} \omega \tau, \quad (1a)$$

where  $\omega$  is the required axle speed in rpm and  $\tau$  is the required torque in Nm. The power provided by the ICE  $P_{ice}$  in W, is then given by

$$P_{ice} = \frac{2\pi}{60} \omega \tau_{ice}(u, \omega), \quad (1b)$$

where  $\tau_{ice}(u, \omega)$  is the total torque provided by the ICE as a nonlinear function of the inputs (fv,  $\dot{m}_{vtg}$ ,  $\dot{m}_{egr}$ ) and engine speed  $\omega$ . Note that since there is no gearbox present and the ICE works in parallel with the EM, the speed of the ICE and EM is fixed by the WHTC. The power supplied by the battery  $P_s$ , is given by

$$P_s = \alpha_2(\omega) P_{em}^2 + \alpha_1(\omega) P_{em} + \alpha_0(\omega), \quad (1c)$$

where  $P_{em}$  is the supplied power by the EM in W and  $\alpha_2(\omega)$ ,  $\alpha_1(\omega)$  and  $\alpha_0(\omega)$  are engine-speed-dependent parameters. The combined power of the ICE and EM should then provide the total required power, i.e.,

$$P_{req} = P_{ice} + P_{em}. \quad (1d)$$

Table 1. Model parameters

Parameter name	Symbol	Unit	Value
Specific heat capacity exhaust gas	$C_{\text{exh}}$	$JK^{-1}kg^{-1}$	1000
Total heat capacity EAS	$C_{\text{EAS}}$	$JK^{-1}$	19500
Ambient heat transfer coefficient	$h_{\text{amb}}$	$JK^{-1}s^{-1}$	15
Ambient temperature	$T_{\text{amb}}$	$K$	293
Number of cylinders	$n_{\text{cyl}}$	-	6
Stoichiometric ratio Adblue / NOx	$\nu$	-	2.007
Crossover temperature	$T_c$	$K$	525
Volume of the EAS	$V_{\text{EAS}}$	$m^3$	0.033
Mass density of the exhaust gas	$\rho_{\text{exh}}$	$kg\ m^{-3}$	1.210

### 2.3 Battery and Aftertreatment System Dynamics

In this paper, we choose the state and the input vectors as

$$x = [E_s \ T_{\text{EAS}} \ m_{\text{NOx,tp}}]^\top, \quad u = [P_s \ \text{fv} \ \dot{m}_{\text{vtg}} \ \dot{m}_{\text{egr}}]^\top, \quad (2)$$

respectively, where  $E_s$  is the stored energy relative to the start of the cycle in kWh,  $T_{\text{EAS}}$  is the temperature of the EAS in K,  $m_{\text{NOx,tp}}$  is the total emitted mass of NOx from the tailpipe in kg,  $P_s$  is the power supplied from the battery in W,  $\text{fv}$  is the amount of fuel injected in the engine in mg/inj,  $\dot{m}_{\text{vtg}}$  is the mass flow resulting from the VTG in kg/s and  $\dot{m}_{\text{egr}}$  is the mass flow resulting from the EGR in kg/s. Following (Donkers et al., 2017; Kessels et al., 2010), the dynamics can be represented in discrete time as  $x_{k+1} = f(x_k, u_k, \omega_k)$  with

$$f(x, u, \omega) = \begin{bmatrix} x^{(1)} - u^{(1)} \\ x^{(2)} + k_1(T_{\text{amb}} - x^{(2)}) + k_2 \dot{m}_{\text{exh}}(u, \omega)(T_{\text{exh}}(u, \omega) - x^{(2)}) \\ x^{(3)} + \dot{m}_{\text{NOx,eo}}(u, \omega)(1 - \eta_{\text{EAS}}(x, u, \omega)) \end{bmatrix}, \quad (3)$$

in which  $k_1 = h_{\text{amb}}/C_{\text{EAS}}$  and  $k_2 = C_{\text{exh}}/C_{\text{EAS}}$ , and where  $\dot{m}_{\text{exh}}(u, \omega)$  and  $\dot{m}_{\text{NOx,eo}}(u, \omega)$  are the exhaust mass flow and NOx engine-out mass flow, respectively, in kg/s,  $T_{\text{exh}}(u, \omega)$  is the exhaust gas temperature in K, and  $\eta_{\text{EAS}}(x, u, \omega)$  is the NOx conversion efficiency. Descriptions of all constants together with their respective values can be found in Table 1. Note that  $x^{(r)}$  represents the  $r$ -th element of the state vector  $x$  and not  $x$  to the  $r$ -th power. This notation is also used for the inputs  $u$ .

### 2.4 Function Approximations

In this paper, function approximations are made based on given lookup tables of a Heavy-Duty ICE. The physical parameters are given in Table 1 and all other constants can be found in Table 2. These functions describe the fuel consumption

$$\dot{m}_f(u, \omega) = \frac{\omega}{60} \frac{n_{\text{cyl}}}{2} u^{(2)} \cdot 10^{-6}, \quad (4)$$

where  $n_{\text{cyl}}$  is the number of cylinders present in the ICE, the exhaust mass flow rate

$$\dot{m}_{\text{exh}}(u, \omega) = \dot{m}_f(u, \omega) + u^{(3)}, \quad (5)$$

i.e., the exhaust gas consists of fuel and the VTG mass flow, the exhaust gas temperature

$$T_{\text{exh}}(u, \omega) = \frac{1}{2} \bar{u}^\top Q_{\text{exh}} \bar{u}, \quad (6)$$

where  $\bar{u} = [\omega \ u^{(2)} \ u^{(3)} \ u^{(4)} \ 1]^\top$  and  $Q_{\text{exh}}$  is a square matrix whose entries are given Table 2. The engine-out NOx emissions are given by

$$\dot{m}_{\text{NOx,eo}}(u, \omega) = c_0 + a_f(u^{(2)} - c_f)^2 + b_f(u^{(2)} - c_f) + a_\omega(\omega - c_\omega)^2 + b_\omega(\omega - c_\omega) + a_{\text{ev}}e^{(b_e(u^{(4)} - c_e) + b_v(u^{(3)} - c_v))}, \quad (7)$$

Table 2. Parameters used for the function approximations

NOx engine out					
$a_f$	$1.327 \cdot 10^{-9}$	$b_f$	$-8.663 \cdot 10^{-7}$	$c_f$	8.244
$a_\omega$	$1.363 \cdot 10^{-10}$	$b_\omega$	$-2.220 \cdot 10^{-7}$	$c_\omega$	863.1
$a_{\text{ev}}$	$9.975 \cdot 10^{-4}$	$b_e$	-14.29	$c_e$	0.238
$c_0$	$1.881 \cdot 10^{-4}$	$b_v$	8.706	$c_v$	0.05
Entries of $Q_{\text{exh}}$ for exhaust temperature					
$q_{11}$	$-2.796 \cdot 10^{-4}$	$q_{22}$	$-3.407 \cdot 10^{-3}$	$q_{34}$	7793
$q_{12}$	$1.773 \cdot 10^{-3}$	$q_{23}$	-3.066	$q_{35}$	-957.6
$q_{13}$	-1.561	$q_{24}$	-5.170	$q_{44}$	2185
$q_{14}$	-0.1673	$q_{25}$	1.815	$q_{45}$	-2776
$q_{15}$	1.023	$q_{33}$	5582	$q_{55}$	-484.2
Entries of $Q_{\text{ice}}$ for ICE Torque					
$q_{11}$	$-6.988 \cdot 10^{-3}$	$q_{22}$	$-3.5070 \cdot 10^{-2}$	$q_{34}$	$-1.417 \cdot 10^4$
$q_{12}$	$-8.056 \cdot 10^{-3}$	$q_{23}$	20.5113	$q_{35}$	-9355
$q_{13}$	9.635	$q_{24}$	11.5247	$q_{44}$	$-2.560 \cdot 10^4$
$q_{14}$	13.90	$q_{25}$	19.15	$q_{45}$	$-1.608 \cdot 10^4$
$q_{15}$	7.043	$q_{33}$	$-2.009 \cdot 10^4$	$q_{55}$	-3592
EAS efficiency					
$s_1$	0.04	$w_1$	0.5061		
$s_2$	0.03	$w_2$	-0.3851		

the torque provided by the ICE is given by

$$\tau_{\text{ice}}(u, \omega) = \frac{1}{2} \bar{u}^\top Q_{\text{ice}} \bar{u}, \quad (8)$$

where  $Q_{\text{ice}}$  is a square matrix whose entries are again given in Table 2, the efficiency of the EAS is given by

$$\eta_{\text{EAS}}(x, u, \omega) = \frac{1}{2} + \frac{1}{\pi} \tan^{-1}(s_1(x^{(2)} - T_c)) + w_1 e^{(h \dot{m}_{\text{exh}}(u, \omega) - 0.5)w_2} \left( \frac{1}{2} - \frac{1}{\pi} \tan^{-1}(s_2(x^{(2)} - T_c)) \right), \quad (9)$$

with  $h = \frac{3600 \cdot 10^{-4}}{V_{\text{EAS}} \rho_{\text{exh}}}$ , and where  $T_c$  is the so called crossover temperature,  $V_{\text{EAS}}$  is the volume of the EAS and  $\rho_{\text{exh}}$  is the mass density of the exhaust gas, and the Adblue consumption is given by

$$\dot{m}_a(x, u, \omega) = \nu \eta_{\text{EAS}}(x, u, \omega) \dot{m}_{\text{NOx,eo}}(u, \omega), \quad (10)$$

where  $\nu$  is the stoichiometric ratio between Adblue and NOx. All the function approximations leads to an maximum full-scale error of less than 5%.

### 2.5 Optimal Control Problem Formulation

After obtaining all the models, the CEEM optimal control problem can be formulated. The goal of the CEEM problem is to minimize the cumulative fuel consumption, i.e.,

$$J = \sum_{k \in \mathcal{K}} \dot{m}_f(u_k, \omega), \quad (11a)$$

where  $\mathcal{K} = \{0, \dots, K-1\}$  is the set containing all time steps, where  $K$  is the length of the cycle, subject to

$$x_0^{(1)} - x_K^{(1)} \leq 0, \quad (11b)$$

which states that the vehicle is required to be, at least, charge sustaining over a given drive cycle (we do not consider battery capacity constraints), and to

$$x_K^{(3)} \leq C_{\text{NOx}}, \quad (11c)$$

where  $C_{\text{NOx}} = M_{\text{NOx}} E_d \cdot 10^{-3}$  poses a limit on the total tailpipe NOx emissions, in which  $M_{\text{NOx}}$  is the constraint on NOx emissions posed by legislation in g/kWh and  $E_d$  is the total required energy/work in kWh, and to

$$P_{\text{ice},k} + P_{\text{em},k} \geq P_{\text{req},k}, \quad (11d)$$

for all  $k \in \mathcal{K}$ , which describes the power balance between the ICE and the EM, and to

$$\underline{u}(\omega_k) \leq u_k \leq \bar{u}(\omega_k), \quad (11e)$$

for all  $k \in \mathcal{K}$ , which bounds the available inputs based on the engine-speed, and to the non-linear dynamics

$$x_{k+1} = f(x_k, u_k, \omega_k), \quad (11f)$$

which are already given in (3).

### 2.6 Extensions

Several extensions can be made to the problem defined above. Some possible extensions are discussed next.

*Zero-Emission Zones:* In the near future, ZEZs will be introduced, in which the ICE is required to be switched off and all required power needs to be supplied by the EM. This can be incorporated into the problem above by adding the constraint  $P_{ice,k} = 0$  for all  $k \in \mathcal{K}_{ZEZ}$ , which implies  $P_{em,k} = P_{req,k}$ , where  $\mathcal{K}_{ZEZ}$  contains all time steps in the ZEZ.

*Local Emission Constraints:* Besides ZEZ, also in-service conformity is required, which states that emissions also need to be constrained on intervals within the drive cycle. To constrain these emissions, an additional constraint can be added

$$x_b^{(3)} - x_a^{(3)} \leq C_{NOx,zone}, \quad (12)$$

where  $a$  and  $b$  denote the time steps at the beginning and the end of a given zone, respectively, where these zones could be determined by a certain amount of energy/work the powertrain requests.

*Adblue Cost:* Since besides fuel, the vehicle also consumes Adblue, the cost function (11a) can be altered to

$$J = \sum_{k \in \mathcal{K}} \pi_f \dot{m}_f(u_k) + \pi_a \dot{m}_a(x_k, u_k), \quad (13)$$

where  $\pi_f$  and  $\pi_a$  are the fuel and Adblue price in €/kg respectively. The addition of the Adblue consumption causes the state  $x_k$ , to be present in the cost function, which increases the complexity of the optimization problem.

## 3. SQP APPROACH

In this section, the Sequential Quadratic Programming (SQP) algorithm that is used to solve the optimal control problem as given in (11) is presented. SQP aims to solve non-linear optimization problems by recursively solving linearly constrained quadratic programs, which is done by approximating the objective function quadratically and the constraints linearly. At the end of this section, we will reflect on the termination condition and the convergence properties of SQP.

### 3.1 Formulation of the SQP Problem

The problem given in (11) can be represented by the optimal control problem

$$\min_{x_k, u_k} \sum_{k \in \mathcal{K}} g(u_k, \omega_k) \quad (14a)$$

$$\text{s.t. } x_{k+1} = f(x_k, u_k, \omega_k) \quad (14b)$$

$$h(x_k, u_k, \omega_k) \leq 0. \quad (14c)$$

Note that for the problem given in (11), the objective function is actually linear. This means that the only non-linearities are within the dynamics and the inequality

constraints. SQP works by recursively solving the optimal control problem

$$\{x_k^{i+1}, u_k^{i+1}\}_{k \in \mathcal{K}} =$$

$$\arg \min_{x_k, u_k} \sum_{k \in \mathcal{K}} \frac{1}{2} (u_k - u_k^i)^\top R (u_k - u_k^i) + g(u_k, \omega_k), \quad (15a)$$

subject to the linearized dynamics

$$x_{k+1} = f(x_k^i, u_k^i, \omega_k) + \nabla f(x_k^i, u_k^i, \omega_k) \begin{bmatrix} x_k - x_k^i \\ u_k - u_k^i \end{bmatrix}, \quad (15b)$$

and to the linearized inequality constraints

$$h(x_k^i, u_k^i, \omega_k) + \nabla h(x_k^i, u_k^i, \omega_k) \begin{bmatrix} x_k - x_k^i \\ u_k - u_k^i \end{bmatrix} \leq 0, \quad (15c)$$

where  $i$  denotes the current iteration of the algorithm and the matrix  $R$  represents the regularization term, which is used to help the algorithm converge in a quicker and more stable manner. The matrix  $R$  is chosen as a nonnegative diagonal matrix, which penalizes the difference in the current en next solution. This leads to better convergence of the SQP algorithm. Moreover, it prevents nonconvexity of the cost function for the case where Adblue consumption is added, i.e., when (13) is considered. By choosing the regularization matrix  $R$  sufficiently large, the QP subproblem becomes convex. When the algorithm converges to a solution, e.g.  $x_k^i = x_k^{i+1} = x^*$  and  $u_k^i = u_k^{i+1} = u^*$ , the solution of the QP subproblem (15) is equal to the solution of the original problem (14).

To arrive at a form for (15) that can be implemented, e.g., in MATLAB, we will introduce a compact notation for (15b), which allows for eliminating the state from (15c). This process is known as ‘condensing’ (Maciejowski, 2001). This process uses a prediction model of the form

$$X = \Phi^i + \Gamma^i U, \quad (16)$$

where  $X = [x_0^\top x_1^\top \dots x_K^\top]^\top$  and  $U = [u_0^\top u_1^\top \dots u_{K-1}^\top]^\top$ , and where  $\Phi^i = (\mathcal{A}^i)^{-1} \mathcal{C}^i$  and  $\Gamma^i = (\mathcal{A}^i)^{-1} \mathcal{B}^i$  with

$$\mathcal{A}^i X = \mathcal{B}^i U + \mathcal{C}^i, \quad (17a)$$

where

$$\mathcal{A}^i = \begin{bmatrix} I & 0 & \dots & 0 \\ -A_0^i & I & 0 & \vdots \\ \vdots & \ddots & \ddots & 0 \\ 0 & \dots & -A_{K-1}^i & I \end{bmatrix}, \mathcal{B}^i = \begin{bmatrix} 0 & \dots & 0 \\ B_0^i & \ddots & \vdots \\ \vdots & \ddots & 0 \\ 0 & \dots & B_{K-1}^i \end{bmatrix}, \mathcal{C}^i = \begin{bmatrix} x_0 \\ C_0^i \\ \vdots \\ C_{K-1}^i \end{bmatrix}, \quad (17b)$$

where  $A_k^i = \nabla_x f(x_k^i, u_k^i, \omega_k)$ ,  $B_k^i = \nabla_u f(x_k^i, u_k^i, \omega_k)$  and  $C_k^i = f(x_k^i, u_k^i, \omega_k) - \nabla f(x_k^i, u_k^i, \omega_k) \begin{bmatrix} x_k^i \\ u_k^i \end{bmatrix}$  follow from the linearized dynamics (15b). Now substituting (16) in (15c) then yields a static optimization problem given by

$$U^{i+1} = \arg \min_U \frac{1}{2} U^\top Q U + G^i U \quad (18a)$$

$$\text{s.t. } H^i U \leq b^i, \quad (18b)$$

where  $Q = \text{diag}(R, \dots, R)$ , and

$$G^i = [0 \ \alpha(\omega_0) \ 0 \ 0 \ \dots \ 0 \ \alpha(\omega_{K-1}) \ 0 \ 0] - U^i Q, \quad (19a)$$

with  $\alpha(\omega_k) = \frac{\omega_k}{60} \frac{n_{cyl}}{2} \cdot 10^{-6}$ , and where

$$H^i = \begin{bmatrix} H_{\text{charge}}^i \\ H_{\text{NOx}}^i \\ H_{\text{pwr},0}^i \\ \vdots \\ H_{\text{pwr},K-1}^i \\ H_{\text{bnds},0}^i \\ \vdots \\ H_{\text{bnds},K-1}^i \end{bmatrix}, \quad b^i = \begin{bmatrix} b_{\text{charge}}^i \\ b_{\text{NOx}}^i \\ b_{\text{pwr},0}^i \\ \vdots \\ b_{\text{pwr},K-1}^i \\ b_{\text{bnds},0}^i \\ \vdots \\ b_{\text{bnds},K-1}^i \end{bmatrix}, \quad (19b)$$

give the linear constraints resulting from (15c) where

$$H_{\text{charge}}^i = [1 \ 0 \ 0] [I_3 \ 0_{3 \times 3(K-2)} \ -I_3] \Gamma^i, \quad (20a)$$

$$b_{\text{charge}}^i = [1 \ 0 \ 0] [-I_3 \ 0_{3 \times 3(K-2)} \ I_3] \Phi^i, \quad (20b)$$

represent the charge sustaining constraint,

$$H_{\text{NOx}}^i = [0 \ 0 \ 1] [0_{3 \times 3(K-1)} \ I_3] \Gamma^i, \quad (20c)$$

$$b_{\text{NOx}}^i = C_{\text{NOx}} - [0 \ 0 \ 1] [0_{3 \times 3(K-1)} \ I_3] \Phi^i, \quad (20d)$$

represent the constraint on NOx emissions,

$$H_{\text{pwr},k}^i = -\nabla(P_{\text{ice}}(u_k^i) + P_{\text{em}}(u_k^i)), \quad (20e)$$

$$b_{\text{pwr},k}^i = -\nabla(P_{\text{ice}}(u_k^i) + P_{\text{em}}(u_k^i))u_k^i + P_{\text{ice}}(u_k^i) + P_{\text{em}}(u_k^i) - P_{\text{req},k}, \quad (20f)$$

give the linear approximation of the power-balance constraint, and

$$H_{\text{bnds},k}^i = \begin{bmatrix} I_4 \\ -I_4 \end{bmatrix}, \quad b_{\text{bnds},k}^i = \begin{bmatrix} \bar{u}(\omega_k) \\ -\underline{u}(\omega_k) \end{bmatrix} \quad (20g)$$

give the bounds on the inputs. The subproblem in (18) can then be solved by any QP solver. We will use IBM CPLEX in this paper.

### 3.2 Convergence and Termination

Due to the iterative nature of the SQP approach, as (14) is solved repeatedly, convergence needs to be monitored and a criterion for termination needs to be formulated. A typical approach is to employ a merit function of the form

$$J^i = \sum_{k \in \mathcal{K}} g(u_k^i, \omega_k) + \mu \max\{h(x_k^i, u_k^i, \omega_k), 0\}, \quad (21)$$

where  $\mu > 0$  is a constant weighting factor. The merit function consists of is the original cost function with an added penalty for any violated constraints. This is necessary as intermediate solutions (of the linearized problem) can be infeasible when evaluated on the original problem. The merit function (21) expresses this by returning a high cost compared to feasible solutions, thereby avoiding convergence to an infeasible solution. It should be noted that only the non-linear constraints need to be included in the merit function since the linear constraints are not altered in the QP subproblem. The SQP algorithm is terminated when  $|J^{i+1} - J^i| \leq \Delta_{\text{tol}}$ , where  $\Delta_{\text{tol}}$  is a specified tolerance.

When the SQP algorithm converges, it is guaranteed that the resulting solution is a local optimum (Nocedal and Wright, 2006). Convergence to the global solution, however, cannot be guaranteed because the CEEM problem is not a convex optimization problem. To assess whether the SQP gets stuck in a local minimum, we initialize the problem with several different initial conditions. Even though a global solution cannot be guaranteed, we have encountered only a few cases where different initial condition converged to different final solutions and we will reflect on this in the next section.

## 4. SIMULATION RESULTS

In this section, the results of the simulation study for the CEEM problem as given in Section 2 are presented. First, the convergence of the SQP algorithm is presented and discussed after which the optimal solution is given and the tradeoff between fuel cost and NOx emissions is shown, where it should again be noted that the drive

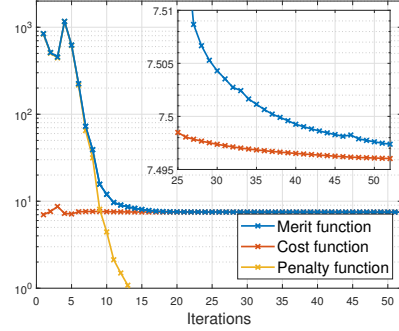


Fig. 3. The cost, penalty and the merit function using  $R$ .

cycle has only positive torques, meaning that the tradeoff is a consequence of thermal management and not of regenerative braking. Lastly, the extensions to the problem regarding local emission zones and Adblue consumption are presented, where in the latter case the combination of fuel cost and AdBlue cost is considered.

### 4.1 Convergence and Tuning

Fig. 3 shows the convergence of the Sequential Quadratic Programming (SQP) algorithm over a given number of iterations when the regularization matrix  $R$  is set as

$$R = \text{diag}(6.67 \cdot 10^{-14}, 2.50 \cdot 10^{-7}, 2.083, 4.20). \quad (22)$$

These values have been obtained by starting with the reciprocal of  $\max_{\omega} \{\bar{u}^{(i)}(\omega)\}$  and then iteratively scaling the elements one by one until a satisfactory convergence rate was achieved. From Fig. 3 it can be seen that the merit function (21) converges quickly to a low value in 25 iterations, after which it continues to decrease slowly until the desired tolerance is achieved. It can be seen from the evolution of the penalty on the constraints (i.e., the second term in (21)) in Fig. 3 that the solutions of the first iterations are infeasible for the nonlinear optimal control problem, and after these become feasible, the cost function (i.e., the first term in (21)) decreases further. Eventually the algorithm converges after 52 iterations which took 309 seconds. On average, iterations take 6.6 seconds and the algorithm converges within 100 iterations and, hence, the worst-case total required time is estimated to be around 11 minutes, which is much lower than the computation times reported in (Donkers et al., 2017) to solve a very similar problem.

### 4.2 Optimal Solution

Fig. 4 shows the optimal solution for the CEEM problem obtained using the SQP problem for  $M_{\text{NOx}} = 0.4$  g/kWh. From Fig. 4a, it can be seen that the optimal strategy is to instantly charge the battery by providing more power than required by the ICE and storing this energy in the battery using the EM. Even though this temporarily emits more NOx, see Fig. 4c, it also does heat up the EAS, see Fig. 4b, which increases its efficiency. This results in severely reduced NOx emissions from the tailpipe after the EAS reaches a temperature greater than 550 K. The stored energy in the battery is then used to operate the ICE in a (close to) optimal operating point, whilst keeping the EAS on a desired temperature. The mentioned initial solution, i.e., the solution at the first iteration of the SQP, is the

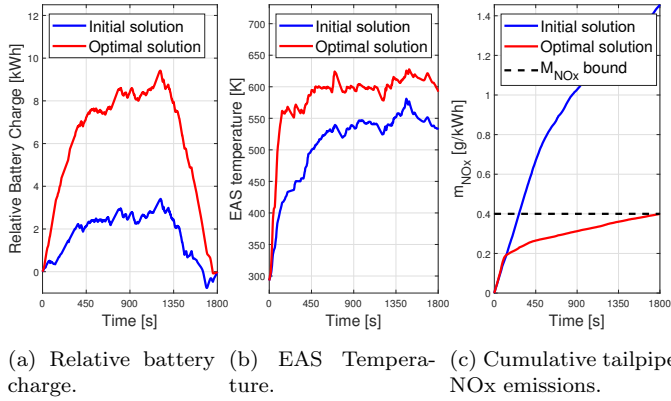


Fig. 4. Optimal solution for  $M_{NO_x} = 0.4g/kWh$ .

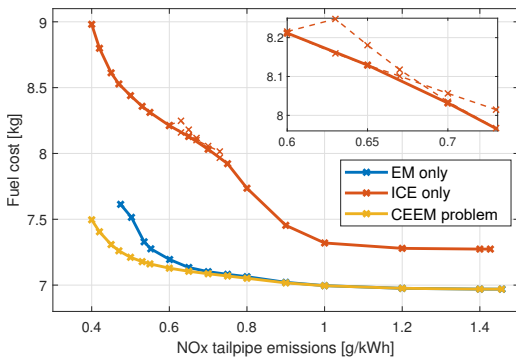


Fig. 5. Cost/ $NO_x$  trade-off for three different cases.

solution obtained from running the algorithm without an emission constraint, e.g., the most fuel efficient solution.

Since multiple simulations have been done for different values of  $M_{NO_x}$ , a trade-off curve can be made showing the increase in cost for lower  $NO_x$  emissions, see Fig. 5. This curve has also been generated for the case that the inputs of the VTG and EGR are chosen such that the ICE is operating at maximum efficiency, and the CEEM strategy can only choose the EM power (EM only), and for the case where the EM cannot be used, which corresponds to the case studied in (Donkers et al., 2017) (ICE only). From Fig. 5, it can be clearly seen that the optimal solution relies heavily on the choice of EM power and less on choosing the VTG and ERG mass flows. This is due to the biggest impact being made by increasing the combination of exhaust gas temperature and mass flow, which can be done relatively cheap using the EM and the battery. This is because charging the battery requires a higher ICE power, which generates more heat, which is partially transferred to the EAS leading to an increased EAS temperature. Without the use of the EM and for low  $NO_x$  tailpipe emissions, EAS temperature is created by producing more power than required for the drive cycle, as (11d) is solved as an inequality, meaning that energy is lost and, hence, results in higher fuel costs.

To assess whether the obtained solutions are global solution (which cannot be guaranteed as the problem is non-convex), different initial conditions are used to see if they converge to the same solution. In the ICE-only case, multiple initial solutions sometimes converge to different (local) minima. As indicated in Fig. 5, for  $M_{NO_x} \in [0.6, 0.73]$ ,

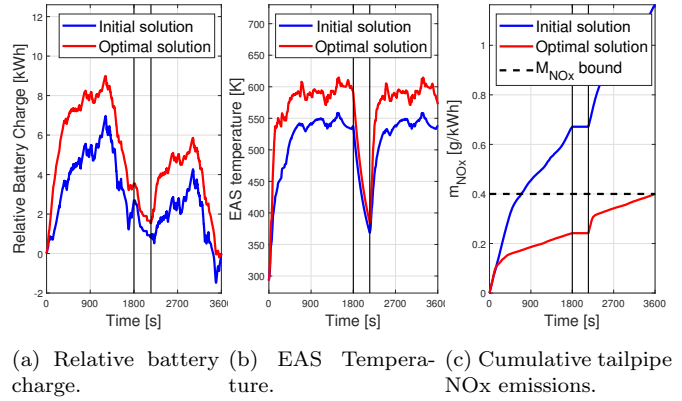


Fig. 6. Optimal solution for  $M_{NO_x} = 0.4g/kWh$  for a double WHTC cycle and where the ICE is switched off from  $t = 1800$  to  $t = 2150$ .

multiple local minima can be found. Note that this effect was only observed for the ‘ICE only’ case for the specified  $M_{NO_x}$  values. The results from Fig. 5 were obtained by using the solution of a previous run with a given  $M_{NO_x}$  value as the initial solution for the next run. By doing this for both increasing and decreasing values of  $M_{NO_x}$ , the dotted lines in Fig. 5 are obtained. Hence, for this case, local optimal solutions exist and the initial condition of SQP should be carefully chosen.

### 4.3 Extensions

Let us now show the results of the proposed extensions in Section 2.6. To demonstrate the consequence of a ZEZ and local emission constraints, a double WHTC cycle is considered, where it is assumed that the ICE has to be switched off and the EM provides all the required power from  $t = 1800$  [s] to  $t = 2150$  [s]. The optimal solution returned by the SQP algorithm is shown in Fig. 6, where the vertical black lines denote the section where the ICE is switched off. It can be seen that no emissions are generated in the time interval from  $t = 1800$  [s] to  $t = 2150$  [s], but, besides that, the optimal solution looks very similar to the optimal solution of the baseline case. As before, the EAS is heated by the charging of the battery, see Fig. 6a and Fig. 6b. It can also be seen that the EAS temperature plummets when driving in the ZEZ, which results in higher  $NO_x$  emissions immediately outside of the ZEZ, see Fig. 6c. This effect is even better visible when the  $NO_x$  emissions are given for smaller zones in Fig. 7, the blue lines, where it is clear that the majority of the emitted mass of  $NO_x$  is emitted when the EAS is (relatively) cold.

To prevent high  $NO_x$  emissions when the EAS is cold, constraints can be added to individual zones, see (12). The length of each zone is chosen so that the cumulative power request in all zones are equal (where the zone inside the ZEZ and the one just after are combined). These constraints are indicated using black dotted lines and the optimal solution in presence of these constraints is shown in red in Fig. 7. It can be observed that the  $NO_x$  emissions from the ‘cold’ zones are spread out more towards neighbouring zones. It does, however, need to be noted that it was not found possible to decrease the cold zones much further than the indicated values in Fig. 7. As



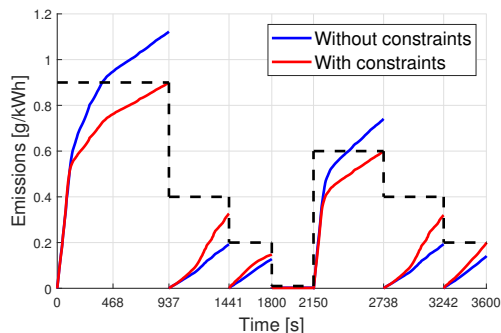


Fig. 7. Local emissions for the optimal solution for  $M_{NO_x} = 0.4g/kWh$  for a double WHTC cycle and where the ICE is switched off from  $t = 1800$  to  $t = 2150$ .

a result of these local NOx emission constraints, the fuel cost increases by 2.8% for this specific simulation example.

So far, only fuel cost has been considered in the CEEM problem, see (11). While fuel cost is not the only operating cost, the optimization problem was also run with the inclusion of Adblue to the objective function, see (13). Table 3 shows a comparison of the total costs for the cases with and without incorporating AdBlue consumption in the objective function. The prices of fuel and AdBlue are also included in the table and it should be noted that we do not consider a ZEZ nor local emission constraints here. It can be seen from Table 3 that the operation cost is hardly reduced by adding AdBlue consumption to the objective function as a decrease in cost of only 0.005% is observed. At the same time, the problem does become more complex since adding Adblue to the problem results in the state occurring in the cost function. This increases the computation times for the QP solver severely resulting in the average time required to solve the CEEM problem going up to three hours which is an entire order of magnitude larger than for the case where AdBlue cost is not considered, yet still faster than DP, as was done in (Donkers et al., 2017).

## 5. CONCLUSION

In this paper, a Combined Energy and Emission Management (CEEM) problem with cold-start conditions over the World Harmonized Transient Cycle (WHTC) was solved using a Sequential Quadratic Programming (SQP) algorithm. This solution was obtained using quasistatic powertrain models and a dynamic after-treatment model, where several lookup-tables have been approximated with smooth functions, resulting in a non-linear discrete-time optimal control problem. It has been shown that SQP is a viable method for solving the CEEM problem since the solution is obtained in a reasonable amount of computation time. Extending the problem with a zero-emission zone, local emission constraints and the addition of AdBlue costs also does not cause any problems to the convergence of the algorithm.

Table 3. Comparison in cost for the optimal solution with and without Adblue optimization.

$M_{NO_x} = 0.6g/kWh$	Without Adblue	With Adblue
Fuel Cost (€1.617 per kg)	€11.53014	€11.53199
Adblue Cost (€0.687 per kg)	€ 0.20319	€ 0.20077
Total Cost	€11.73334	€11.73276

The simulation results show the well-known trade off between the operating cost of the vehicle and the amount of nitrogen oxides (NOx) emitted from the tailpipe. By comparing the NOx-cost tradeoff of the three considered cases, it can be concluded that most of the benefits of CEEM come from the electric machine and much less is achieved with the regulation of the mass flows within the internal combustion engine (ICE). Finally, adding AdBlue costs in the problem formulation leads to 0.005% lower costs, whilst it does add significantly to the complexity of the problem. These topics should be taken into consideration when going to a real-time implementable solution to the problem.

## REFERENCES

- Ao, G.Q., Qiang, J.X., Zhong, H., Mao, X.J., Yang, L., and Zhuo, B. (2008). Fuel economy and NOx emission potential investigation and trade-off of a hybrid electric vehicle based on dynamic programming. *Proc Institution of Mechanical Eng, Part D*.
- Demirgok, B., Thiruvengadam, A., Pradhan, S., Besch, M., Thiruvengadam, P., Posada, F., Quiros, D.C., and Hu, S. (2021). Real-world emissions from modern heavy-duty vehicles: Sensitivity analysis of in-use emissions analysis methods. *Atmospheric Environment*.
- Donkers, M., van Schijndel, J., Heemels, W., and Willems, F. (2017). Optimal control for integrated emission management in diesel engines. *Control Engineering Practice*.
- Holmer, O., Willems, F., Blomgren, F., and Eriksson, L. (2020). Optimal Aftertreatment Pre-Heat Strategy for Minimum Tailpipe NOx Around Green Zones. *SAE Technical paper*.
- Kessels, J., Willems, F., Schoot, W., and van den Bosch, P. (2010). Integrated Energy & Emission Management for Hybrid Electric Truck with SCR aftertreatment. In *Proc Vehicle Power & Propulsion Conf*.
- Khalik, Z., Padilla, G., Romijn, T., and Donkers, M. (2018). Vehicle Energy Management with Ecodriving: A Sequential Quadratic Programming Approach with Dual Decomposition. In *Proc American Control Conf*.
- Maciejowski, J.M. (2001). *Predictive Control with Constraints*. Pearson.
- Muncrief, R. (2015). Comparison of real - world off-cycle NOx emissions control in Euro IV , V , and VI. Technical report, Int Council On Clean Transportation.
- Nocedal, J. and Wright, S.J. (2006). *Numerical Optimization*. Springer, New York, NY.
- Onori, S. and Serrao, L. (2011). On Adaptive-ECMS strategies for hybrid electric vehicles. In *Int Scientific Conference on Hybrid & Electric Vehicles*.
- Pérez, L.V., Bossio, G.R., Moitre, D., and García, G.O. (2006). Optimization of power management in a hybrid electric vehicle using dynamic programming. *Mathematics & Computers in Simulation*.
- Pisu, P. and Rizzoni, G. (2007). A Comparative Study of Supervisory Control Strategies for Hybrid Electric Vehicles. *IEEE Trans Control Syst Technology*.
- Willems, F., Spronkmans, S., and Kessels, J. (2011). Integrated Powertrain Control to Meet Low CO2 Emissions for a Hybrid Distribution Truck With SCR-Denox System. In *Proc ASME Dynamic Syst & Control Conf*.